JOURNAL OF MATERIALS SCIENCE 30 (1995) 1333–1337

# Effect on the grain interior and grain boundary reactions by Cr addition to low gold content alloys

I. KAWASHIMA, H. OHNO, Y. ARAKI
*Department of Dental Materials Science, School of Dentistry, Health Sciences University of Hokkaido, 1757, Kanazawa, Ishikari-Tobetsu, Hokkaido, Japan*

The effect on grain interior and grain boundary reactions by Cr addition to low gold content alloys were investigated by electric resistivity measurements, hardness tests, optical microscopic observations, and TEM observations. The grain interior reactions were accelerated by the chromium addition while grain boundary reactions were retarded. The formation of AuCu I type ordered phase in the grain interior was accelerated, and the T–T–T curve of AuCu I type ordered phase shifted to higher temperatures and shorter times with increasing chromium content.

## 1. Introduction

Low gold content alloys which contain more gold than usual Ag–Pd–Cu alloys, possess high corrosion resistance. A previous paper has shown that grain interior reactions in Ag–Pd–Cu alloys with 40 mass% Au are effectively retarded [1]. The increase in hardness of alloys with 40% Au is caused by the appearance of AuCu I type ordered phase in the grain interior [2]. The grain interior hardening reaction in Ag–25 mass% Pd–10% Cu alloy is accelerated by adding Cr. The increase in hardness of the low gold content alloy is also caused by the appearance of AuCu I type ordered phase in the grain interior [3]. Therefore, it is hoped that grain interior hardening reactions in low gold content alloys may be accelerated by addition of Cr.

In this paper, the effects of Cr addition on the grain interior and grain boundary reactions of 40 mass% Au alloys were investigated by electrical resistivity measurements, hardness tests, optical microscopic observations, X-ray diffraction (XRD), and transmission electron microscopic (TEM) observations.

## 2. Materials and methods

Table I shows the composition (mass%) of the alloys (40Au–25Pd–23.5 to 25Ag–10Cu) with 0, 0.5, 1.0 and 1.5% Cr. The alloys were prepared from metals of purity better than 99.9% in an alumina Tamman tube under an argon atmosphere in a high frequency induction furnace, and then cast in a stainless steel mould. The melted mass of each alloy was 50 g. The weight loss in the melting process was less than 0.1% and a chemical analysis after the melting was not carried out. The ingots were cold worked slightly and homogenized at 900 °C for 4 h. Block specimens, $5 \times 5 \times 10$ mm, for optical microscopic observations and hardness measurements, and $1\phi \times 100$ mm wire specimens for electrical resistivity measurements were prepared by cold working. For the solution treatment the specimens were kept at 900 °C for 2 h before quenching in ice water. The specimens were finally aged at 350 °C or 400 °C in a salt bath. Electrical resistivity with isothermal ageing was measured by the four terminal potentiometric method with a direct current of 100 mA at room temperature. Hardness tests were performed with a 25 g load by a micro-Vickers hardness tester. The hardness values were averages of ten indentations. Identification of phases were made by XRD. The XRD measurements were conducted as follows: the target was Cu with a 35 kV tube voltage and 20 mA current. 3 mm diameter discs were punched out of heat-treated thin foil specimens, and electrothinned to transparency by a double-jet technique prior to TEM observations.

TABLE I Nominal composition of alloys (mass%)

| | Au | Pd | Cu | Ag | Cr |
|---|---|---|---|---|---|
| No. 1 | 40.0 | 25.0 | 10.0 | 25.0 | – |
| 2 | 40.0 | 25.0 | 10.0 | 24.5 | 0.5 |
| 3 | 40.0 | 25.0 | 10.0 | 24.0 | 1.0 |
| 4 | 40.0 | 25.0 | 10.0 | 23.5 | 1.5 |

## 3. Results and discussion

### 3.1. Electrical resistivity and hardness with isothermal ageing

Fig. 1a and b show changes in electrical resistivity and hardness for the No. 1–4 alloys aged at 350 °C. In Fig. 1a, $\rho_0$ is the specific resistivity after the solution treatment and $\rho$ that after ageing. The electrical

0022–2461  

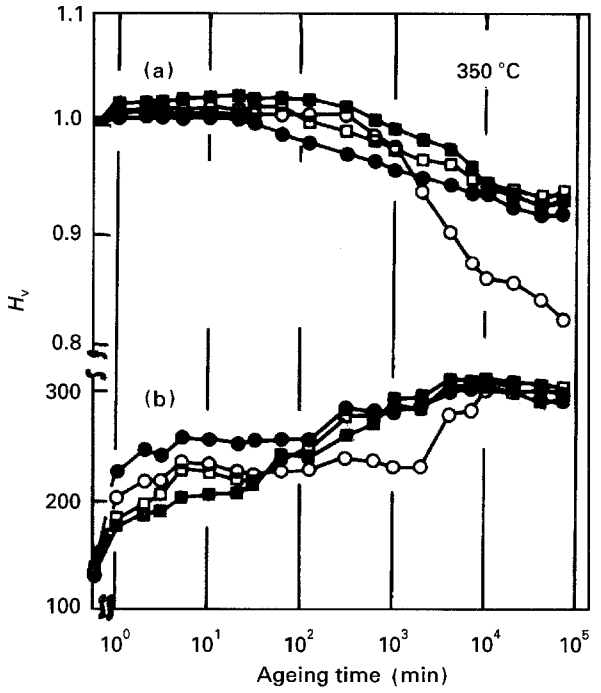


*Figure 1* Electrical resistivity changes (a) and hardness (b) aged at 350 °C on various alloys. ○, 0%; ●, 0.5%; □, 1.0%; ■, 1.5%.

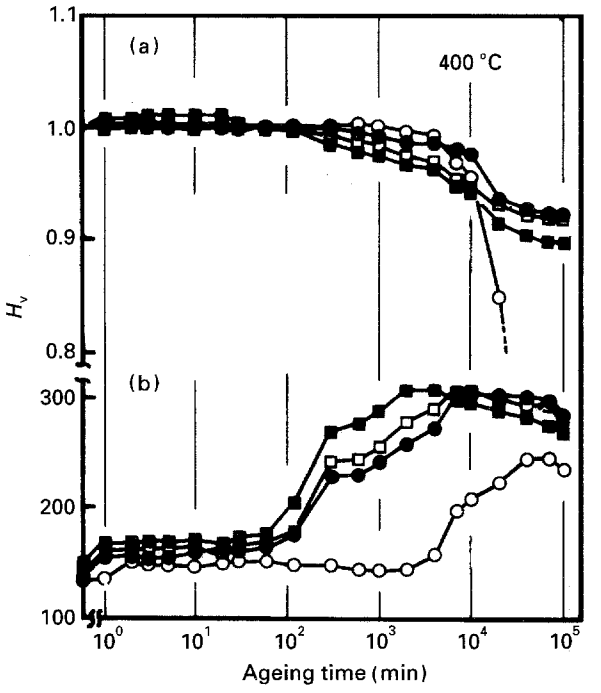


*Figure 2* Electrical resistivity changes (a) and hardness (b) aged at 400 °C. ○, 0%; ●, 0.5%; □, 1.0%; ■, 1.5%.

resistivity curve for No. 1 alloy decreases rapidly from the start of the grain boundary reaction, for the No. 2–4 alloys the decrease is not so rapid. The grain interior precipitation reactions after 300 min were accelerated by addition of Cr, and the hardness values in the matrix increased ($H_v = 270$).

Fig. 2 shows ageing at 400 °C, here the specific resistivity decreased rapidly from $10^4$ min after the grain boundary reactions started as in the case of ageing at 350 °C. The electrical resistivity curve for the No. 2–4 alloys did not decrease as rapidly as the No. 1 alloy. This indicates that grain boundary precipitates in the alloys with Cr did not appear up to $10^5$ min. The specific resistivity of the alloys aged at 400 °C increased faster with the Cr content than when the ageing treatment was at 350 °C. In Fig. 2b, the No. 1 alloy does not harden until $2 \times 10^3$ min, and the alloys with Cr begin to harden from $10^2$ min and the maximum hardness ($H_v = 300$) is higher than without Cr. Therefore, the grain interior hardening process in the alloys aged at 400 °C is accelerated like the alloys aged at 350 °C.

## 3.2. Optical microstructures

Fig. 3 shows the microstructures of No. 1–4 alloys aged at 400 °C for $4 \times 10^3$ min. Grain boundary precipitates do not appear until this time as may be predicted with Fig. 2a. A precipitate-free zone (PFZ) was observed in No. 1 alloy where the hardness of this area is lower than the values of the grain interior. The striation (Fig. 3b) is produced by the formation of AuCu I type ($L1_0$ type) ordered phase in the grain interior of the No. 2 alloy. The microstructure where the twinning process proceeded steadily to release the coherency strain. While the grain size is small and the precipitate-free zone disappears with increasing Cr content, twins increase in the grain interior (arrows in Fig. 3c and d).

## 3.3. X-ray diffraction

Fig. 4 shows XRD patterns of alloys aged at 400 °C for $4 \times 10^3$ min. The small shoulder at the low angle side of the α phase (fcc) appeared in the XRD patterns of the No. 1 alloy. With higher Cr contents, the grain interior reactions were accelerated and the peak of the AuCu I type ($L1_0$ type) ordered phase appeared with 1.0% Cr. Therefore, it is considered that the striation observed in Fig. 3b appears due to the presence of AuCu I type ($L1_0$ type) ordered phase in the matrix. The grain boundary reaction (β-PdCu, CsCl type + Ag rich-$\alpha_2$, fcc) has not proceeded in the alloys with the heat treatments here, as can also be seen in Fig. 3.

Figs 5 and 6 show the XRD patterns of alloys without Cr (a) and with 1.5% Cr (b) aged at 350 °C (Fig. 5) and 400 °C (Fig. 6) for $4 \times 10^4$ min. The peak intensity of β-PdCu ordered phase of the CsCl type line is strong in (a) at both ageing temperatures, and with 1.5% Cr the peak intensity of AuCu I type ($L1_0$ type) ordered phase line is stronger than the β-PdCu ordered phase of the CsCl type line (b).

## 3.4. TEM observations

Fig. 7 shows the electron diffraction patterns with 1.5% Cr alloys aged at 400 °C for 600 min. In the diffraction pattern long streaks along the ⟨0 0 2⟩ direction and extra spots at 1 1 0 and equivalent positions are visible. From these facts, it is concluded that the hardening in the grain interior is not due to the

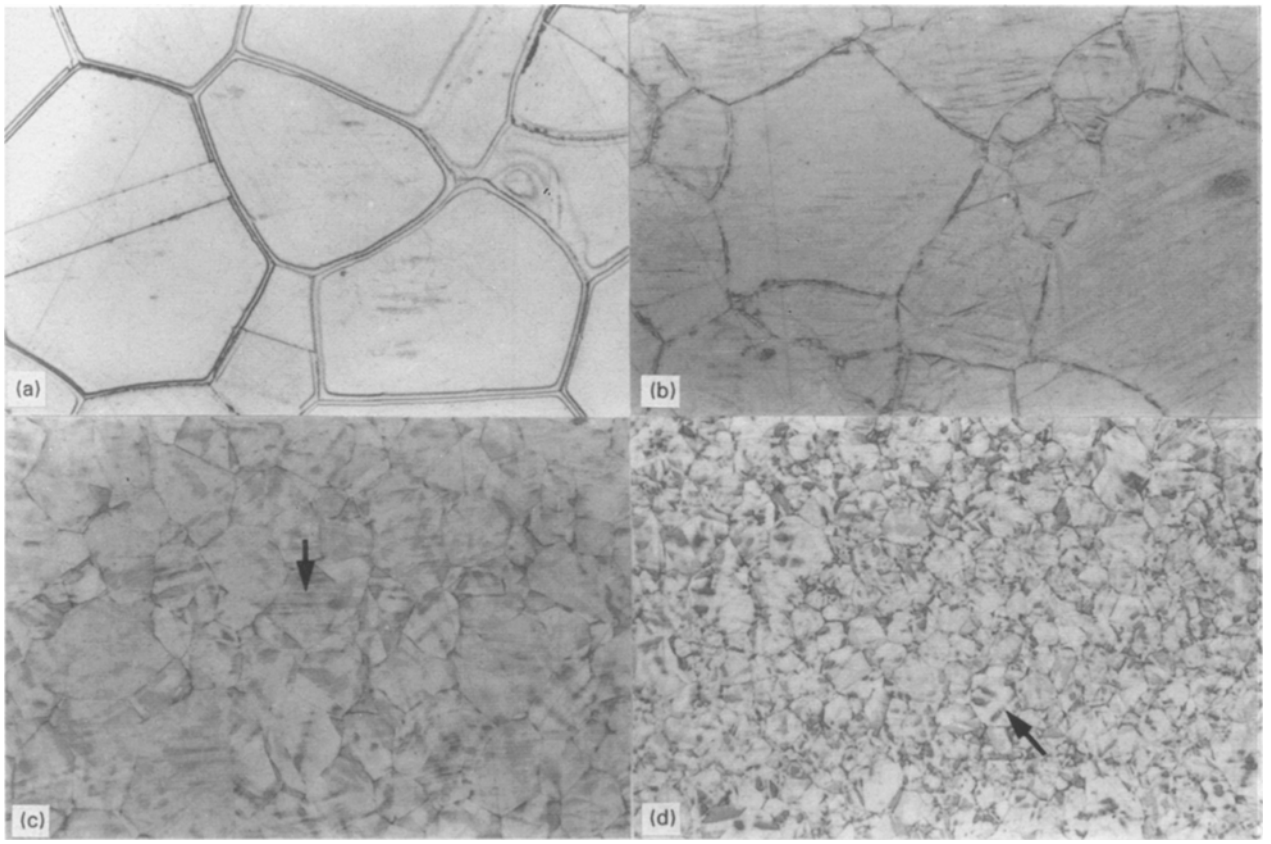


*Figure 3* Microstructure aged at 400 °C for $4 \times 10^3$ min in various alloys. (a) 0% Cr; (b) 0.5 %Cr; (c) 1.0% Cr; (d) 1.5% Cr.

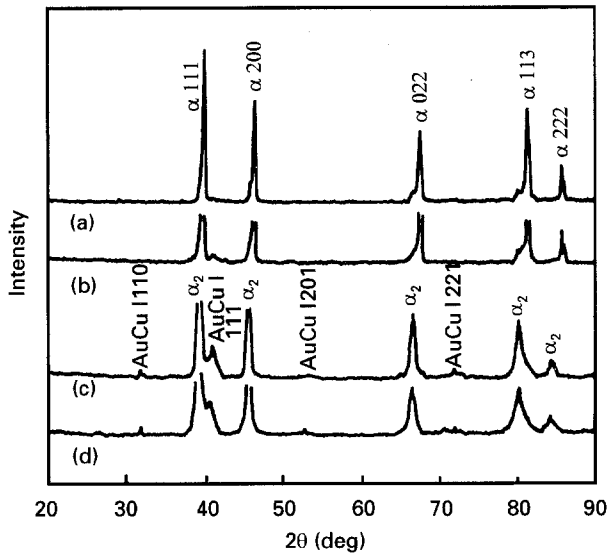


*Figure 4* XRD patterns aged at 400 °C for $4 \times 10^3$ min in various alloys. (a) 0% Cr; (b) 0.5% Cr; (c) 1.0% Cr; (d) 1.5% Cr.

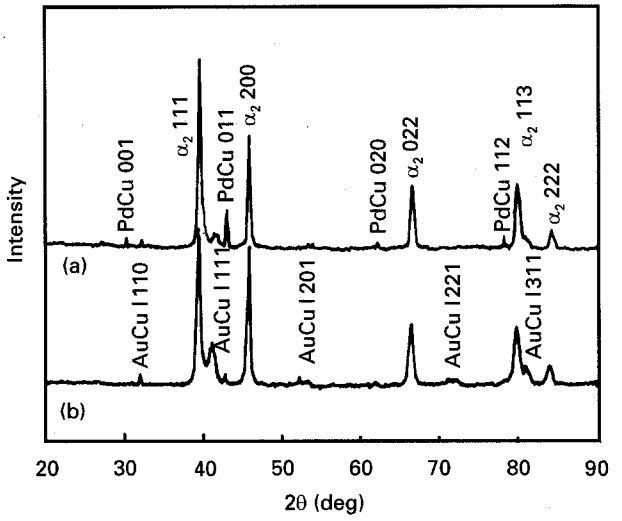


*Figure 5* XRD patterns aged at 350 °C for $4 \times 10^4$ min with no (a) and 1.5% Cr added (b).

formation of intermetallic compounds or solid solution containing Cr but is due to AuCu I type ($L1_0$ type) ordered phase.

## 3.5. Acceleration of grain interior reactions due to Cr addition

Fig. 8 shows the time of appearance of AuCu I type ($L1_0$ type) ordered phase and β-PdCu ordered phase of the CsCl type which was obtained from the XRD patterns of the various alloys. The time of appearance of each phase was obtained from the time when the 1 0 0 peak for AuCu I ordered phase and the 1 1 0 peak for the β-PdCu ordered phase of CsCl type begin to appear. The T–T–T curve of the AuCu I type ($L1_0$ type) ordered phase shifts to shorter times and higher temperatures with Cr content while the curve of the β-PdCu ordered phase of CsCl type shifts to longer times with increasing Cr content. The critical temperatures of the β-PdCu ordered phase of CsCl type are

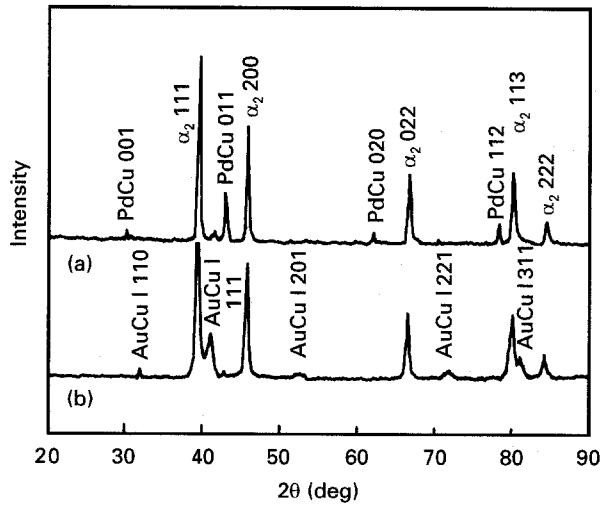


*Figure 6* XRD patterns aged at 400 °C for $4 \times 10^4$ min with no (a) and 1.5% Cr added (b).

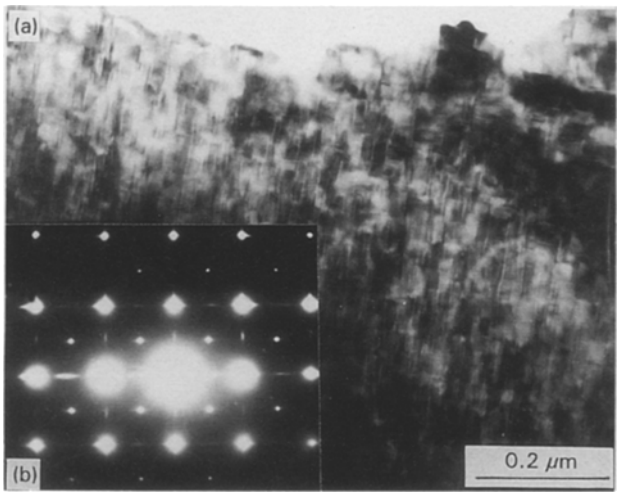


*Figure 7* Transmission electron micrograph and electron diffraction pattern in 1.5% Sn adding alloy aged at 400 °C for 600 min. (a) Bright field area; (b) diffraction pattern.

500 °C for the binary Pd–Cu system and the ageing temperatures are lower than that. The age-hardening process in alloys with Cr was caused by accelerated formation of AuCu I type ordered phase. Therefore, as shown by the T–T–T curve for AuCu I type ordered phase the age-hardening process was initiated earlier with increasing Cr content.

### 3.6. Retardation of grain boundary reactions due to Cr addition

As previously reported [4], the electrical resistivity (Fig. 2) decreases rapidly from the start of the grain boundary reaction ($10^4$ min) in the Cr-free alloys. As can be seen, the electrical resistivity decreased to $\rho/\rho_0 = 0.9$ and became constant with Cr, grain boundary reactions did not occur up to $10^5$ min. There are two main mechanisms by which element additions retard grain boundary reactions:

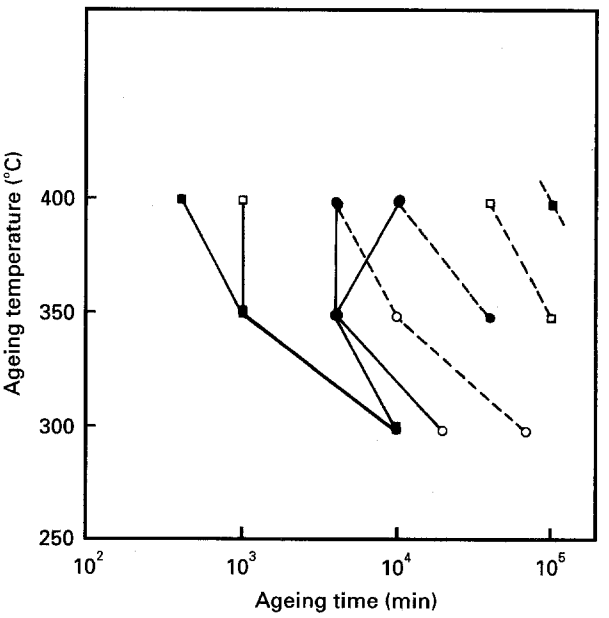


*Figure 8* T–T–T diagram in various alloys: solid line shows appearance of AuCu I type superlattice and dashed line shows the appearance of CsCl type superlattice. ○, 0%; ●, 0.5%; □, 1.0%; ■, 1.5%.

1. The chemical driving force for the grain boundary reaction becomes low when the added element accelerates grain interior reactions [6].
2. Movement of the nodule interface becomes small due to segregation or grain interior precipitates [7].

With theory 1, grain interior reactions accelerate by addition of Cr, as can be seen in Fig. 2b. With theory 2, as can be seen in Fig. 3, the grain size decreases and recrystallization was retarded with Cr addition. As the solution treatments for all the alloys are the same, the hysteresis of both the working treatment and the heat treatments are also the same. As the alloys do not transform when they are solution-treated, the movement of the grain boundaries reflects the grain size after the solution treatment. This leads to the conclusion that the mobility of the grain boundary decreases with Cr addition. As a result, it may be concluded that the grain boundary reaction is retarded as a result of both theory 1 and 2.

## 4. Conclusions

The effect of Cr addition on grain interior and grain boundary reactions of alloys containing 40 mass% Au were investigated by electrical resistivity measurements, hardness tests, optical microscopic observations, XRD and TEM observations.

1. Grain interior reactions accelerate, and grain boundary reactions were retarded with Cr addition.
2. The appearance of AuCu I type ordered phase was accelerated, and that of β-PdCu ordered phase (CsCl type) was retarded with increasing Cr content.

3. The T–T–T curve of the AuCu I type ($L1_0$ type) ordered phase shifts to higher temperatures and shorter times with increasing Cr content.

## References


1. I. KAWASHIMA, Y. KANZAWA, Y. ARAKI and H. OHNO, *J. Jpn Inst. Metals* **53** (1989) 14.
2. M. OHTA, K. HISATSUNE and M. YAMANE, *J. Jpn Soc. Dent. Appar. Mater.* **16** (1975) 87.
3. I. KAWASHIMA, Y. ARAKI and H. OHNO, *J. Mater. Sci.* **26** (1991) 1113.
4. M. OHTA, T. SHIRAISHI, K. HISATSUNE and M. YAMANE, *J. Less Common Metals* **59** (1980) 1966.
5. H. ISAKA, *J. Jpn Soc. Dent. Appar. Mater.* **28** (1977) 137.
6. A. H. GEISLER, "Phase Transformation in Solids" (John Wiley and Sons, 1951) p. 432.
7. M. MIKI and Y. OGINO, *J. Jpn Inst. Metals* **48** (1984) 347.



*Received 28 September 1993*
*and accepted 5 September 1994*